

## ORIGINAL ARTICLE

# Spinal sample showing p-JNK and P38 associated with the pain signaling transduction of glial cell in neuropathic pain

J Cao<sup>1</sup>, J-s Wang<sup>2</sup>, X-h Ren<sup>1</sup> and W-d Zang<sup>1</sup>**Objective:** To investigate the signaling pathways after astrocytes were activated in neuropathic pain.**Methods:** Thirty-six Sprague Dawley (s.d.) rats were randomly divided into two groups (each group with 18 s.d. rats) including chronic constriction injury (CCI) of the sciatic nerve model group and sham operation group. Operation was performed on the right leg in all rats. The lumbar spinal cord (L4 and L5) was taken to make paraffin slices on the 1st day before operation and the 1st, 3rd, 7th, 14th and 28th day after operation in each group. Paraffin slices were labeled with p38 mitogen-activated protein kinase (p38MAPK) and c-Jun N-terminal kinase (JNK) by immunofluorescence staining, and then were co-labeled with hexaribonucleotide binding protein-3 (NeuN), glial fibrillary acidic protein (GFAP) and anti-integrin  $\alpha$ M (CD11b) antibody (OX-42) to explore the associations of p38MAPK and JNK with nerve cells or glial cell.**Results:** Compared with sham group, the pain threshold was significantly decreased, and astrocyte-activated markers, GFAP and vimentin were significantly increased in CCI group. The mean fluorescence intensities of p38MAPK and JNK were increased in the right spinal dorsal horn of CCI group. The coexpression of JNK and GFAP was found in astrocytes of the spinal dorsal horn in CCI group.**Conclusion:** JNK signal transduction pathway is involved in the pain signaling transduction of astrocytes.*Spinal Cord* (2015) **53**, 92–97; doi:10.1038/sc.2014.188; published online 11 November 2014

## INTRODUCTION

There has not been an effective therapy for neuropathic pain because its pathogenesis is not completely clear. The treatment for neuropathic pain is a major clinical challenge. However, it is reported that spinal glial cells are associated with the pathogenesis of pain.<sup>1</sup> Both microglia and astrocytes are activated in the spinal cord after nerve injury.<sup>2</sup> Glial cells not only act as various receptors of neurotransmitters, but also can produce many inflammatory mediators such as interleukin-1 $\beta$ , interleukin-6, tumor necrosis factor- $\alpha$  and prostaglandin E2 that lead to painful sensitization.<sup>3</sup> Spinal microglia is important for the occurrence of neuropathic pain.<sup>4</sup> Although astroglia cells are persistently activated in the spinal cord after nerve injury, the role of glial subtype in hyperalgesia is not completely clear.

The mitogen-activated protein kinases (MAPKs), a family of evolutionally conserved molecules, have a critical role in cell signaling and gene expression.<sup>5,6</sup> MAPK family consists of three major members, including extracellular signal-regulated kinase, p38 and c-Jun N-terminal kinase (JNK), which are three different signaling cascades.

Unexpectedly, p38 is not activated both in hexaribonucleotide binding protein-3 (NeuN)-expressing neurons and in glial fibrillary acidic protein (GFAP)-expressing astrocytes after spinal nerve ligation, but is activated in anti-integrin  $\alpha$ M (CD11b) antibody (OX-42)-expressing microglia.<sup>7</sup>

Recently, a selective and permeable peptide inhibitor of JNK and D-JNKI-1 is more potent than SP600125 in alleviating neuropathic pain.<sup>8</sup> JNK is involved in inflammatory pain, but little research report shows that JNK is involved in neuropathic pain.

In this study, we made chronic constriction injury (CCI) models, and explored the signal transduction pathway of astrocytes and the role of JNK in regulating neuropathic pain using immunohistochemistry.

## MATERIALS AND METHODS

All study methods were approved by the Ethics Committee of the First Affiliates Hospital of Zhengzhou University.

### Preparation of CCI models

Thirty-six 2-month aged male Sprague Dawley rats weighing between 180 and 220 g lived in a 12-h light–dark cycle and were given access to food and water *ad libitum*. They were kept under the conditions for 1 week before operation. The 36 Sprague Dawley rats were randomly divided into two groups including CCI group and sham operation group (each group with 18 Sprague Dawley rats). CCI models were prepared as follows: after intraperitoneal anesthesia with 10% chloral hydrate (3 ml kg<sup>-1</sup>), Sprague Dawley rats were in prone position. The right thigh skin was disinfected with povidone–iodine solution followed by making a cut. The biceps femoris was isolated to expose the sciatic nerve. Four mild ligation rings with each interval length of 1–2 mm around the nerve was made with nonabsorbed surgical suture (6–0 nylon). Appropriate ligation strength could allow the calf muscle to produce mild fibrillation. Finally, the incision was closed with silk thread.<sup>4</sup> In sham group, only the right sciatic nerve was exposed, and then the incision was closed.

### Pain behavior assays

Mechanical withdraw threshold (MWT) was tested with Von Frey (Stoelting, Wood Dale, IL, USA) to evaluate mechanical allodynia and paw withdrawal thermal latency (PWTL) was measured to evaluate thermal hyperalgesia.<sup>9</sup> MWT

<sup>1</sup>Department of Anatomy, Medical College, Zhengzhou University, Zhengzhou, China and <sup>2</sup>Department of Anatomy, Luohe Medical College, Luohe, China  
Correspondence: Dr W-d Zang, Department of Anatomy, Medical College, Zhengzhou University, Number 100, Science Road, Zhengzhou 450001, China.  
E-mail: zwd@zzu.com

Received 23 January 2014; revised 11 September 2014; accepted 28 September 2014; published online 11 November 2014

was first tested followed by measurement of PWTL in all rats on the 1st day before operation and the 1st, 3rd, 7th, 14th and 28th day after operation in 0800–1000 h. (1) MWT was tested using Von Frey filaments (Stoeling). For each time, 0.02 g was forced onto the plantar surface of the foot with a filament. The percentages of negative responses were calculated for each foot. (2) PWTL measurement method: heat hyperalgesia was evaluated using Plantar Test (UgoBasile, Comerio, Italy). To ensure accuracy, the Plantar Test apparatus had been calibrated before PWTL was measured. A mobile heat source with an infrared intensity of 70 was placed under the hind paw. PWTL was defined as the duration from giving radiant heat to inducing paw withdraw. Each foot was measured three times, and then their average was calculated. There was a 5-min rest period between both measurements. Furthermore, each animal was allowed to habituate to the environment for 1 h before any measurements.

**Materials and fix**

Animals were anesthetized with isoflurane, and then perfused through the ascending aorta with saline followed by 4% paraformaldehyde/1.5% picric acid. After the perfusion, the spinal cord segments (L4, L5) and the dorsal root ganglions (DRGs; L4, L5) were collected and fixed in the same fixative for 12 h. Spinal cord tissue was dehydrated with ethanol gradient, embedded in paraffin, and then sliced at a thickness of 4 μm.

**Immunohistochemistry**

These sections were incubated with 3% H<sub>2</sub>O<sub>2</sub> at 37 °C for 20 min, and then with goat serum at 37 °C for 20 min.

Single-labeling immunofluorescence histochemistry was performed as described previously.<sup>10</sup> All primary antisera were purchased from Santa Cruz Biotechnology (Paso Robles, CA, USA). After being blocked for 1 h at 37 °C in phosphate buffered saline (PBS) containing 5% goat serum and 0.3% Triton X-100, the sections were incubated with primary antibodies GFAP and vimentin, or primary antibodies p-p38MAPK and p-JNK overnight at 4 °C, respectively. The sections were then incubated with goat anti-mouse or anti-rabbit IgG conjugated with TRITC (Beijing Zhongshan Golden Bridge Biotechnology Co., Beijing, China) or fluorescein isothiocyanate for 1 h at 37 °C. Control experiments included the primary antiserum with corresponding antigen (Cell Signaling Technology, Danvers, MA, USA), normal rabbit serum with the primary antiserum, and serum without the primary antiserum. Finally, the sections were rinsed in 0.01 M PBS. A mixture of 50% glycerin and 2.5% triethylene diamine in 0.01 M PBS were applied to cover slips. The imaging of the sections was performed with a fluorescence microscope (BX43, Olympus, Tokyo, Japan). Fluorescein isothiocyanate emitted green light under a wavelength of 488 nm and TRITC red light under a wavelength of 550 nm. The obtained fluorescence intensities were statistically analyzed with image2X software (Dallas, TX, USA). The testing was performed in triplicate.

**Double-labeling immunofluorescence histochemistry**

The sections were incubated overnight at 4 °C for 1 h with a mixture of mouse-anti-p-p38MAPK monoclonal antibody (1:100 dilution) and rabbit-anti-NeuN polyclonal antibody (1:100 dilution), or mixture of mouse-anti-p-p38MAPK monoclonal antibody (1:100 dilution) and rabbit-anti-GFAP polyclonal antibody (1:100 dilution), or mixture of mouse-anti-p-p38MAPK monoclonal antibody (1:100 dilution) and rabbit-anti-OX-42 polyclonal antibody (1:100 dilution), or mixture of mouse-anti-p-JNK monoclonal antibody (1:100 dilution) and rabbit-anti-NeuN polyclonal antibody (1:100 dilution), or mixture of mouse-anti-p-JNK monoclonal antibody (1:100 dilution) and rabbit-anti-GFAP polyclonal antibody (1:100 dilution), or mixture of mouse-anti-p-JNK monoclonal antibody (1:100 dilution) and rabbit-anti-OX-42 polyclonal antibody (1:100 dilution), and equivalent volume mixture of goat-anti-rabbit TRITC (1: 100 dilution) and goat-anti-rat fluorescein isothiocyanate (1:100 dilution). Control experiments were performed as previously described in parallel. After the sections were rinsed in 0.01 M PBS, a mixture of 50% glycerin and 2.5% triethylene diamine in 0.01 M PBS were applied to cover slips. All immunofluorescence-labeled sections were observed with an epifluorescence microscope under appropriate filter. The testing was performed in triplicate.

**Statistical analysis**

All data were expressed as  $\bar{x} \pm S$ . Statistical treatment was performed with SPSS 13.0 software (Chicago, IL, USA). Paired data *t*-test was used in the comparison within group, and independent samples *t*-test was used in comparison between groups. Statistical significance was established at *P*<0.05.

**RESULTS**

**Pain behavior changes in CCI rats**

There were no significant differences in both MWT and PWTL between the two groups on the 1st day before operation (*P*>0.05). In the rats of CCI group, after the right sciatic nerve ligation, the right foot toes moved close to each other with dorsiflexion, eversion and lameness. MWT and PWTL of the right foot began decreasing 1 day after operation and reached the peak 7 days after operation in CCI group. MWT and PWTL were significantly lower in right foot of CCI group than in contralateral left foot of CCI group and both feet of sham group on the 3rd, 7th and 14th day after operation (*P*<0.05, Figure 1).

**The expressions of GFAP and vimentin in the spinal dorsal horn**

The immunofluorescence staining only with GFAP or vimentin showed that GFAP or vimentin-positive cells were present in the spinal cord and began increasing after operation in CCI group. The fluorescence intensity of GFAP was increased and was significantly higher in CCI group than in sham and contralateral groups on the 3rd, 7th, 14th and 28th day after operation (*P*<0.05, Figure 2). The fluorescence intensity of vimentin was increased with a peak of 7–14 days after operation and was significantly higher in CCI group than in sham and contralateral groups on the 3rd, 7th, 14th and 28th day

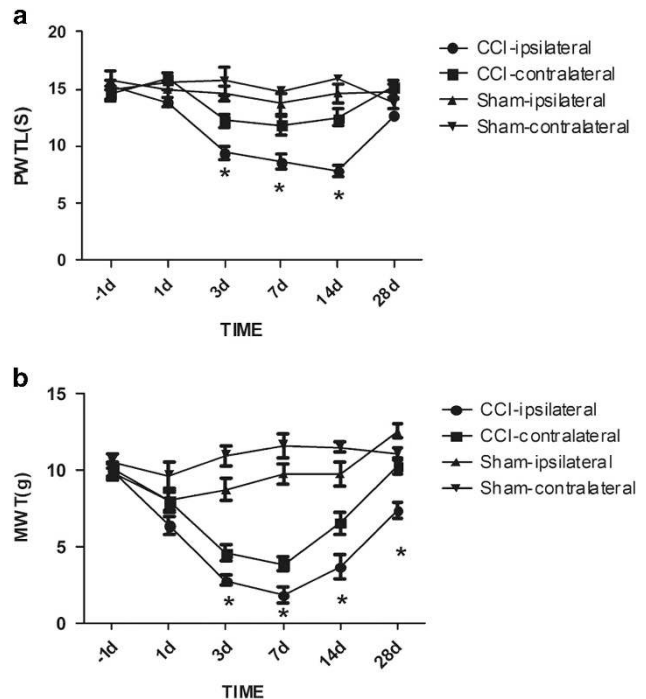


**Figure 1** MWT and PWTL in CCI rat models. (a) MWT measured with Von Frey Filaments. (b) PWTL detected by thermal hyperalgesia. MWT and PWTL values are measured on the 1st day before operation and the 1st, 3rd, 7th, 14th and 28th day after operation at between 0800 and 1000 h in all rats. MWT: mechanical withdraw threshold; PWTL: paw withdrawal thermal latency. Ipsilateral side in CCI group (right side in CCI group).

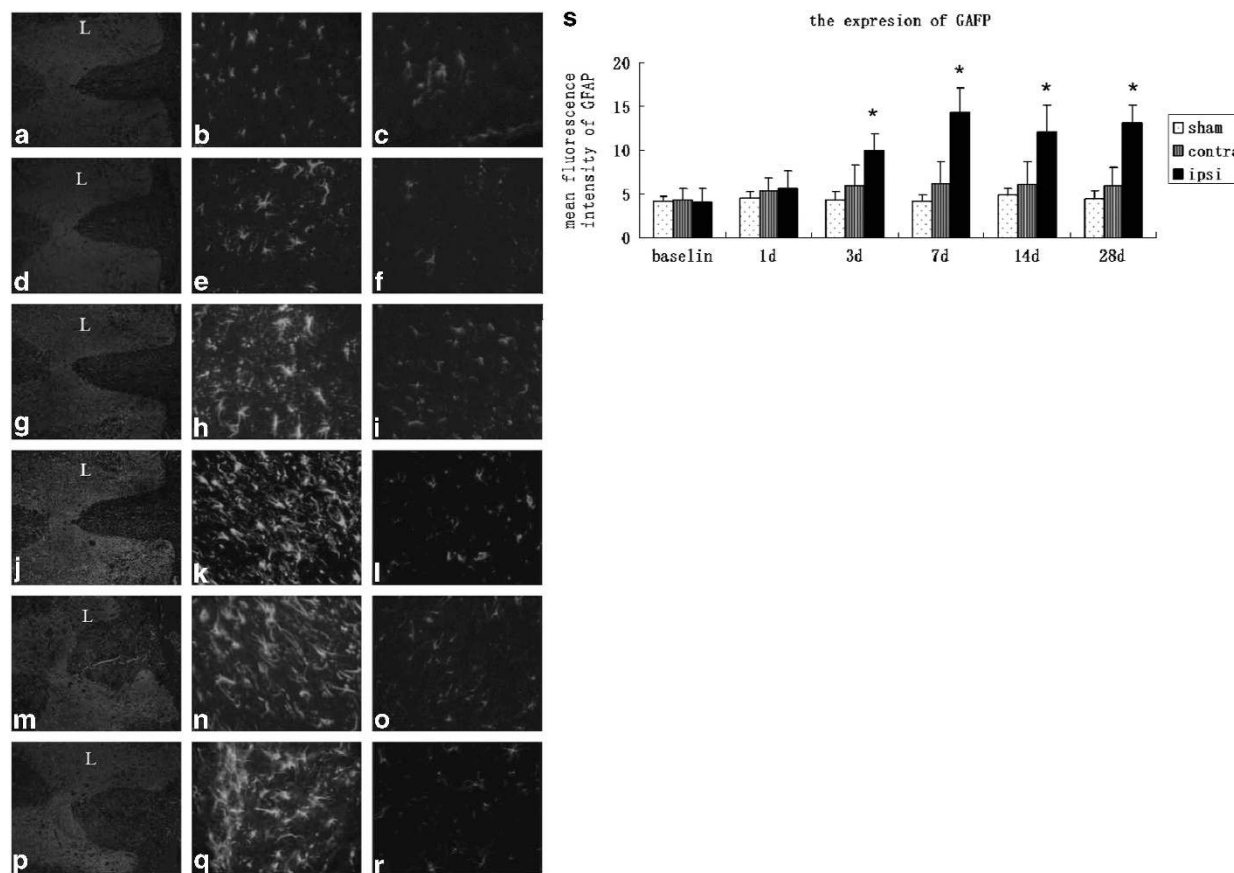


**Figure 2** The expression of GFAP in the spinal dorsal horn CCI group (a and b) and sham group (c) before operation; CCI group (d and e) and sham group (f) 1 day after operation; CCI group (g and h) and sham group (i) 3 days after operation; CCI group (j and k) and sham group (l) 7 days after operation; CCI group (m and n) and sham group (o) 14 days after operation; CCI group (p and q) and sham group (r) 28 days after operation; fluorescence intensity in sham group, contra-side in CCI group and ipsilateral in CCI group (s). a, d, g, j, m and p:  $\times 100$ ; b, c, e, f, h, i, k, l, n, o, q and r: 400. Notes: GFAP: glial fibrillary acidic protein. \* Indicates  $P < 0.05$ , compared with the fluorescence intensity in contra-side and sham groups at the same time. Ipsilateral side (right side in CCI group, CCI group). Contra-side (left side in CCI group, contra-side group). A full color version of this figure is available at the *Spinal Cord* journal online.

after operation ( $P < 0.05$ , Figure 3). Both GFAP- and vimentin-positive signals were mainly present in the cytoplasm.

#### GFAP expressions in DRGs

To observe whether neuropathic pain is associated with peripheral glial cells in DRGs, we performed the immunohistochemistry with GFAP in DRGs. Strikingly, the intensity of GFAP staining was markedly increased in DRGs of CCI models and was significantly higher in CCI group than in sham group on the 7th day after operation ( $P < 0.05$ , Figure 4). We found that the satellite cells around DRG neurons were activated (Figure 4).

#### The expression of p-p38MAPK in CCI group

Immunofluorescence showed that the number of p-p38MAPK-positive cells was higher in CCI group than in contralateral and sham groups on the 7th day after operation, positive cells were large and the fluorescent signals were distributed in the cytoplasm. The fluorescence intensity was significantly higher in CCI group than in sham group on the 7th day after operation ( $P < 0.05$ , Figure 5).

#### The expression of p-JNK in CCI group

Immunofluorescence showed that the number of p-JNK-positive cells was higher in CCI group than in contra-side and sham groups on the

7th day after operation, positive cells were large and the fluorescent signals were distributed in the cytoplasm. The fluorescence intensity was significantly higher in CCI group than in sham group on the 7th day after operation ( $P < 0.05$ , Figure 6).

#### Double immunofluorescence-labeling of p-p38MAPK or p-JNK with NeuN, GFAP or OX-42

The results of double immunofluorescence-labeling p-p38MAPK/NeuN, p-p38MAPK/GFAP and p-p38MAPK/OX-42 showed that there were many coexpression areas on p-p38MAPK/OX-42 labeling section on the 7th day after operation in CCI group. The results of double immunofluorescence-labeling p-JNK/NeuN, p-JNK/GFAP and p-JNK/OX-42 showed that there were many coexpression areas on p-JNK/NeuN labeling section on the 7th day after operation in CCI group (Figure 7).

#### DISCUSSION

It has been recognized that increased GFAP expression means that astrocytes are activated in neuropathic pain.<sup>11</sup> Activated astrocytes directly affect the function of neurons through releasing variety of cellular active factors and neural active substances, having a major role in neuropathic pain.<sup>12</sup> Therefore, in order to block the astrocyte's

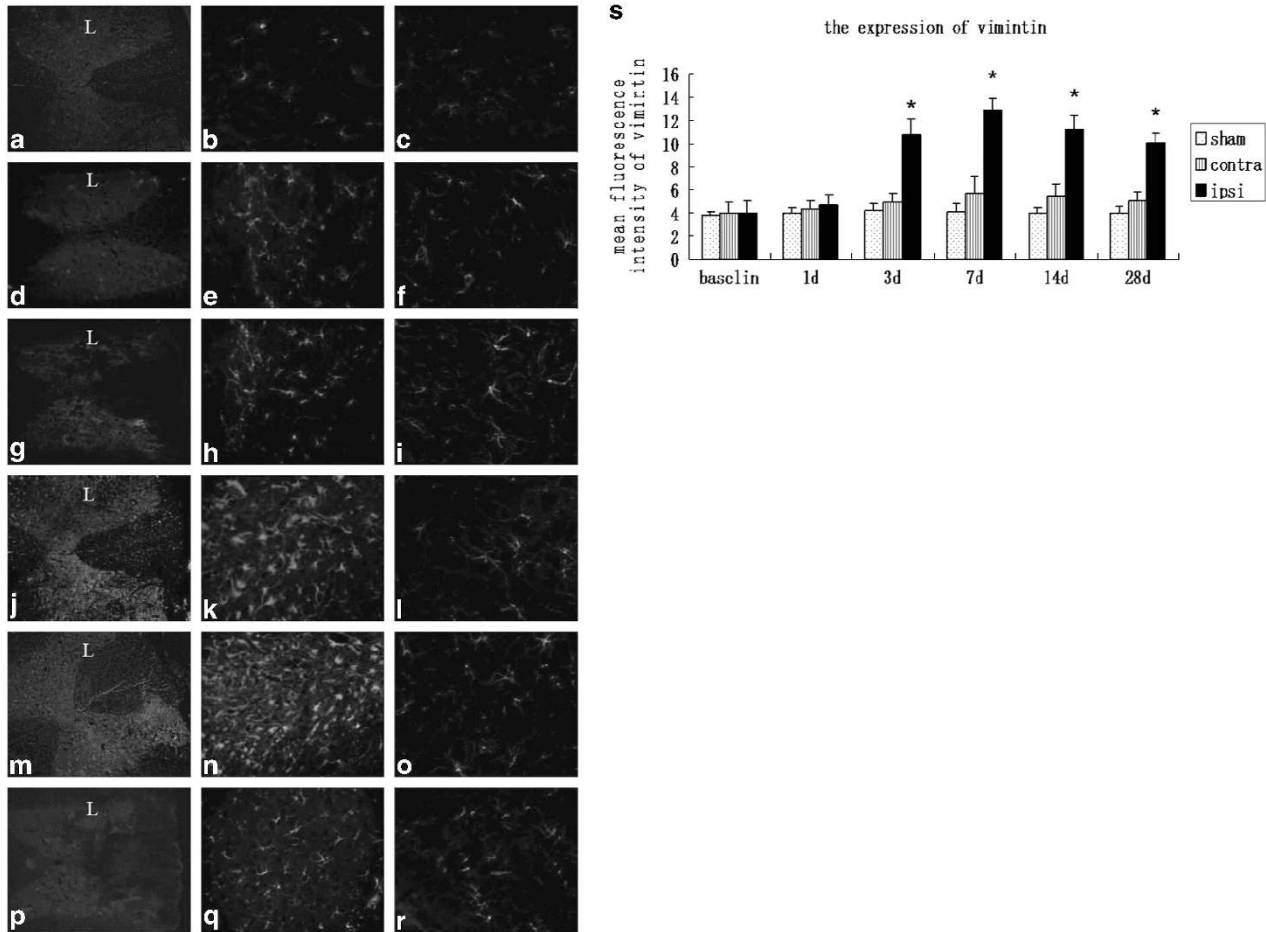


**Figure 3** The expression of vimentin in the spinal dorsal horn. CCI group (a and b) and sham group (c) before operation; CCI group (d and e) and sham group (f) 1 day after operation; CCI group (g and h) and sham group (i) 3 days after operation; CCI group (j and k) and sham group (l) 7 days after operation; CCI group (m and n) and sham group (o) 14 days after operation; CCI group (p and q) and sham group (r) 28 days after operation; fluorescence intensity in sham group, contra-side in CCI group and ipsilateral in CCI group (s). a, d, g, j, m and p:  $\times 100$ ; b, c, e, f, h, i, k, l, n, o, q and r:  $\times 400$ . \* Indicates  $P < 0.05$ , compared with the fluorescence intensity in contra-side and sham groups at the same time. Ipsilateral side (right side in CCI group, CCI group) Contra-side (left side in CCI group, contra-side group). A full color version of this figure is available at the *Spinal Cord* journal online.

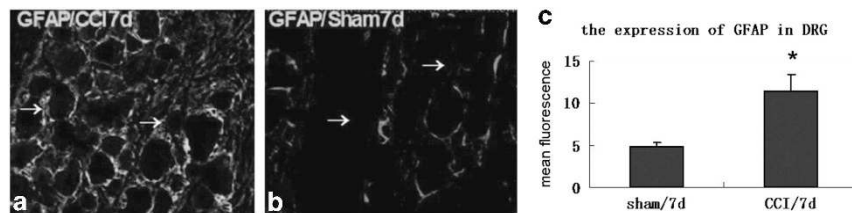


**Figure 4** The expression of GFAP in DRGs on the 7th day after operation. a: GFAP expression in DRGs of CCI group; b: GFAP expression in DRGs of sham group.  $\times 400$ . c: Comparison of GFAP expression in DRGs between CCI group and sham group. \* Indicates  $P < 0.05$ , compared with the fluorescence intensity in sham groups. A full color version of this figure is available at the *Spinal Cord* journal online.

activated process, it is necessary to explore through which signaling pathways, the astrocytes, are activated.

#### p38MAPK and neuropathic pain

p38MAPK is one of the key members of MAPK pathways. In neuropathic pain, p38MAPK can be activated through phosphorylation. The activated p-p38MAPK can activate the transcription factors including ELK-1, ATF-2 and MAX, producing a variety of cytokines that regulate the synthesis of nitric oxide and cell protein, and are

involved in signal transduction and hyperalgesia.<sup>13</sup> However, there have been different reports regarding whether p38MAPK is involved in the pain signal pathway of astrocytes. Ji *et al.*<sup>14</sup> performed double immunofluorescence-labeling of p-p38MAPK with NeuN (neuron-specific recognition protein), GFAP (astrocyte-specific recognition protein) or OX-42 (microglia-specific recognition protein) in spinal nerve ligation model, and found that p-p38MAPK and OX-42 staining areas were consistent; so they believed that the p38MAPK was involved in pain signaling of microglia. However, Wang *et al.*<sup>13</sup>

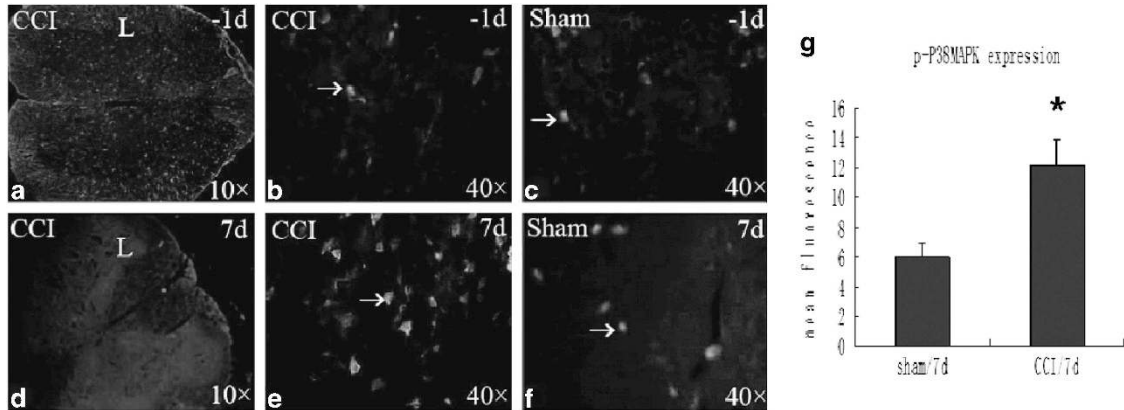


**Figure 5** The expression of p-p38MAPK in the spinal dorsal horn. CCI group (a and b) and sham group (c) before operation; CCI group (d and e) and sham group (f) 7 days after operation; fluorescence intensity in sham group and in CCI group (g). a and d:  $\times 100$ ; b, c, e and f:  $\times 400$ . Arrows indicate p-p38MAPK positive cells. \* Indicates  $P < 0.05$ , compared with the fluorescence intensity in sham group on the 7th day after operation. A full color version of this figure is available at the *Spinal Cord* journal online.

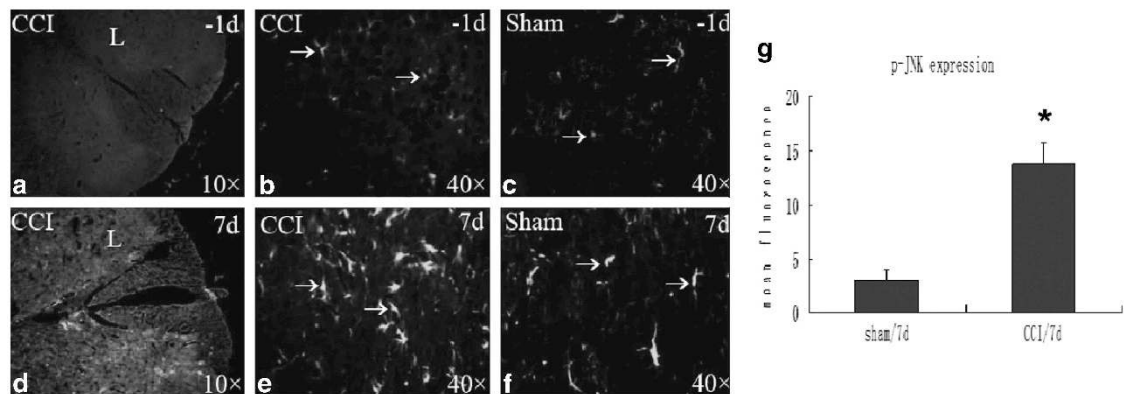


**Figure 6** The expression of p-JNK in the spinal dorsal horn CCI group (a and b) and sham group (c) before operation; CCI group (d and e) and sham group (f) 7 days after operation; fluorescence intensity in sham group and in CCI group (g). a and d:  $\times 100$ ; b, c, e and f:  $\times 400$ . Arrows indicate p-JNK positive cells. \* Indicates  $P < 0.05$ , compared with the fluorescence intensity in sham group on the 7th day after operation. A full color version of this figure is available at the *Spinal Cord* journal online.

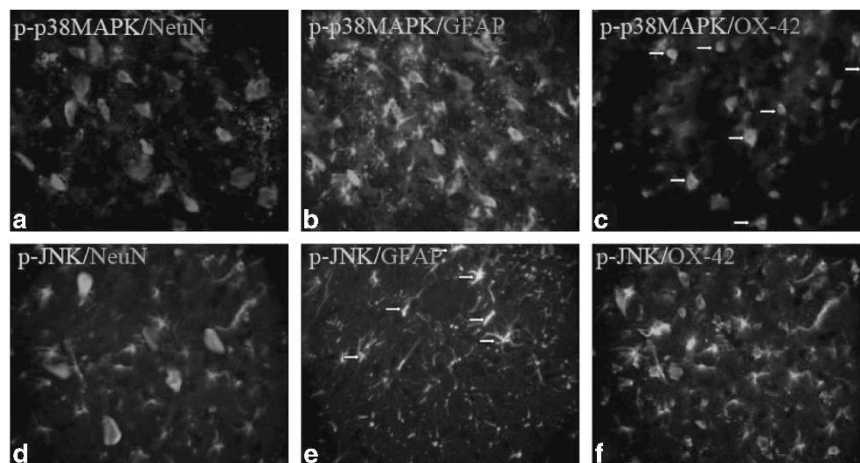


**Figure 7** The sections of the right spinal cord double immunofluorescence-labeling p-p38MAPK or p-JNK with NeuN, GFAP and OX-42 in CCI group on the 7th day after operation,  $\times 400$  p-p38MAPK is green and NeuN red. a: no coexpression in neurons; b: no coexpression in astrocytes; c: coexpression in microglia; d: no coexpression of both in neurons; e: coexpression in astrocytes; f: no coexpression in microglia. Arrows in c and e indicate coexpression. A full color version of this figure is available at the *Spinal Cord* journal online.

reported that after p material activated astrocytes *in vitro*, western blot analysis, reverse transcriptase-PCR and enzyme-linked immunosorbent assay indicated that p38MAPK were activated with high expression, so they believed that p38MAPK's activation was related to astrocytes.

In this study, in the condition that astrocytes were activated in CCI group, immunofluorescence staining of p-p38MAPK alone, and then double immunofluorescence-labeling of p-p38MAPK with NeuN, GFAP or OX-42 were performed. The results showed that the number of p38MAPK immunoreactive cells was increased in the CCI model, and the average fluorescence intensity was strengthened with statistical significance compared with that in sham group, demonstrating that p38MAPK signal transduction pathway is activated. The results of the double immunofluorescence-labeling indicated that there was p-p38MAPK expression in microglia. This confirms that p38-MAPK signal pathway may be involved in pain signaling of microglia.

### JNK and neuropathic pain

JNK is also one of the three main members of MAPK pathways. In neuropathic pain, JNK can be activated after phosphorylation. Zhuang *et al.*<sup>15</sup> found that p-JNK mediated the activation of astrocytes in spinal cord, leading to persistent neuropathic pain. Ji *et al.*<sup>14</sup> described that in preserving nerve injury models, double immunofluorescence-labeling p-JNK and GFAP in the spinal dorsal horn showed their consistent distribution area.<sup>16</sup>

In this study, in the condition that astrocytes were activated in CCI group, immunofluorescence staining of p-JNK alone, and then double immunofluorescent-labeling p-JNK with NeuN, GFAP or OX-42 were performed. The results showed that p-JNK signal transduction pathway was activated in CCI models of neuropathic pain, and its expression area was consistent with that of astrocytes. p-JNK signal pathway may be involved in pain signaling of astrocytes.

In our experiments, we also found that both spinal astrocytes and satellite cells<sup>17</sup> surrounding the dorsal ganglion neurons are activated, markedly enhancing GFAP expression. The interaction between satellite glial cells and dorsal ganglion neurons in the ganglion provides new ideas for further studies.

In conclusion, this study indicates that signal transduction pathways are related to the activation of astrocytes in neuropathic pain, confirms that both p38MAPK and JNK signal pathways are activated in neuropathic pain and shows that only JNK signal pathway is involved in pain signal transduction of astrocytes. This study provides a theoretical basis for further studies on the mechanism of neuropathic pain.

### DATA ARCHIVING

There were no data to deposit.

### CONFLICT OF INTEREST

The authors declare no conflict of interest.

### ACKNOWLEDGEMENTS

This study was supported by the National Natural Science Foundation of China (No. 81171059, 81200866).

- 1 Uga H, Tsuda S. A one-step reverse transcription-polymerase chain reaction system for the simultaneous detection and identification of multiple tospovirus infections. *Phytopathology* 2005; **95**: 166–171.
- 2 Raghavendra V, Tanga FY, DeLeo JA. Attenuation of morphine tolerance, withdrawal-induced hyperalgesia, and associated spinal inflammatory immune responses by propentofylline in rats. *Neuropsychopharmacology* 2004; **29**: 327–334.
- 3 Ji RR, Strichartz G. Cell signaling and the genesis of neuropathic pain. *Sci STKE* 2004; **2004**: reE14.
- 4 Coull JA, Beggs S, Boudreau D, Boivin D, Tsuda M, Inoue K *et al*. BDNF from microglia causes the shift in neuronal anion gradient underlying neuropathic pain. *Nature* 2005; **438**: 1017–1021.
- 5 Lee HJ, Shin YK, Park HT. Mitogen activated protein kinase family proteins and c-jun signaling in injury-induced Schwann cell plasticity. *Exp Neurol* 2014; **23**: 130–137.
- 6 Yang DP, Kim J, Syed N, Tung YJ, Bhaskaran A, Mindos T *et al*. p38 MAPK activation promotes denervated Schwann cell phenotype and functions as a negative regulator of Schwann cell differentiation and myelination. *J Neurosci* 2012; **32**: 7158–7168.
- 7 Hossain S, de la Cruz-Morcillo MA, Sanchez-Prieto R, Almazan G. Mitogen-activated protein kinase p38 regulates Krox-20 to direct Schwann cell differentiation and peripheral myelination. *Glia* 2012; **60**: 1130–1144.
- 8 Zhuang ZY, Kawasaki Y, Tan PH, Wen YR, Huang J, Ji RR *et al*. Role of the CX3CR1/p38 MAPK pathway in spinal microglia for the development of neuropathic pain following nerve injury-induced cleavage of fractalkine. *Brain Behav Immun* 2007; **21**: 642–651.
- 9 Zhu C, Yu ZB, Zhu JG, Hu XS, Chen YL, Qiu YF *et al*. Differential expression profile of micRNAs during differentiation of cardiomyocytes exposed to polychlorinated biphenyls. *Int J Mol Sci* 2012; **13**: 15955–15966.
- 10 Jiang G, Cao F, Ren G, Gao D, Bhakta V, Zhang Y *et al*. PRSS3 promotes tumour growth and metastasis of human pancreatic cancer. *Gut* 2010; **59**: 1535–1544.
- 11 Liu MG, Zhang FK, Guo SW, Zhao LF, An YY, Cui XY *et al*. Phosphorylation of c-Jun N-terminal kinase isoforms and their different roles in spinal cord dorsal horn and primary somatosensory cortex. *Neurosci Lett* 2007; **427**: 39–43.
- 12 Basbaum AI, Braz JM. Transgenic mouse models for the tracing of 'pain' pathways. In: Kruger L, Light AR (eds). *Translational Pain Research: From Mouse to Man*. Frontiers in Neuroscience: Boca Raton, FL. 2010.
- 13 Wang YX, Xu XY, Su WL, Wang Q, Zhu WX, Chen F *et al*. Activation and clinical significance of p38 MAPK signaling pathway in patients with severe trauma. *J Surg Res* 2010; **161**: 119–125.
- 14 Ji RR, Kawasaki Y, Zhuang ZY, Wen YR, Decosterd I. Possible role of spinal astrocytes in maintaining chronic pain sensitization: review of current evidence with focus on bFGF/JNK pathway. *Neuron Glia Biol* 2006; **2**: 259–269.
- 15 Zhuang ZY, Wen YR, Zhang DR, Borsello T, Bonny C, Strichartz GR *et al*. A peptide c-Jun N-terminal kinase (JNK) inhibitor blocks mechanical allodynia after spinal nerve ligation: respective roles of JNK activation in primary sensory neurons and spinal astrocytes for neuropathic pain development and maintenance. *J Neurosci* 2006; **26**: 3551–3560.
- 16 Naik AK, Tandan SK, Dudhgaonkar SP, Jadhav SH, Kataria M, Prakash VR *et al*. Role of oxidative stress in pathophysiology of peripheral neuropathy and modulation by N-acetyl-L-cysteine in rats. *Eur J Pain* 2006; **10**: 573–579.
- 17 Warwick RA, Hanani M. The contribution of satellite glial cells to chemotherapy-induced neuropathic pain. *Eur J Pain* 2013; **17**: 571–580.